




Translation information processing is regulated by protein kinase C-dependent mechanism in Purkinje cells in murine posterior vermis

Rosendo G. Hernández^a, Chris I. De Zeeuw^b, Ruyan Zhang^a, Tatyana A. Yakusheva^{a,1} , and Pablo M. Blazquez^{a,1} 

^aDepartment of Otolaryngology, Washington University, St. Louis, MO 63110; and ^bDepartment of Neuroscience, Erasmus University Medical Center, 3000 DR Rotterdam, The Netherlands

Edited by Ranulfo Romo, National Autonomous University of Mexico, Mexico City, Mexico, and approved June 9, 2020 (received for review February 6, 2020)

The cerebellar posterior vermis generates an estimation of our motion (translation) and orientation (tilt) in space using cues originating from semicircular canals and otolith organs. Theoretical work has laid out the basic computations necessary for this signal transformation, but details on the cellular loci and mechanisms responsible are lacking. Using a multicomponent modeling approach, we show that canal and otolith information are spatially and temporally matched in mouse posterior vermis Purkinje cells and that Purkinje cell responses combine translation and tilt information. Purkinje cell-specific inhibition of protein kinase C decreased and phase-shifted the translation component of Purkinje cell responses, but did not affect the tilt component. Our findings suggest that translation and tilt signals reach Purkinje cells via separate information pathways and that protein kinase C-dependent mechanisms regulate translation information processing in cerebellar cortex output neurons.

spatial navigation | vestibular | posterior vermis | Purkinje cell | cerebellar plasticity

Animals need to correctly estimate their motion and orientation in space to navigate through their environment. In most vertebrates, this is primarily accomplished by combining visual and vestibular sensory information. In some vertebrates, vision could take a secondary role in favor of other sensory modalities (e.g., echolocation in bats), but in all cases, vestibular information is essential for estimating our body position and motion with respect to the world (1). Using information about our motion and orientation in space, the central nervous system (CNS) can estimate our location in space over time, even in the absence of visual information, a process called path integration (2).

To enable path integration, the CNS faces an important computational challenge in that it needs to extract world-centered information (tilt and translation) from vestibular cues sensed by our vestibular organs. One problem is that our biological linear accelerometers (otolith organs) cannot distinguish between gravitational and inertial forces (3, 4). This gives rise to the “tilt/translation ambiguity problem”—our otolith organs respond identically to being tilted and translated (e.g., tilting backward and translating forward; Fig. 1*A*). The second problem is that our biological angular accelerometers (semicircular canals) are not influenced by gravity forces—they respond identically during yaw rotation while upright and yaw rotation while supine. A mathematical solution to the above tilt/translation ambiguity suggests that the gravitational component of the net linear acceleration, detected by the otoliths, could in principle be canceled out by a tilt signal, generated from semicircular canal information (5–7). However, for this computation to work, canal and otolith information must be matched temporally and spatially before they are combined. Importantly, angular head velocity information from the three pairs of semicircular canals must be first transformed into head rotation around the earth horizontal axis and then be integrated to estimate angular position (tilt).

There is ample evidence suggesting that the posterior vermis of the cerebellar cortex (nodulus and ventral uvula; below referred to as NU) plays an essential role in spatial navigation, specifically in the computation of translation and tilt. Physiological and anatomical studies have shown that the cerebellum is functionally connected with the hippocampal formation (8–11). Moreover, NU receive information from otoliths and semicircular canals afferents (12–14) and output an estimation of tilt and translation (15, 16). Disruption of cerebellar function by overexpression of an inhibitor of protein kinase C (PKC) specifically in Purkinje cells (L7-PKCI mice), which among other effects prevents induction of postsynaptic long-term depression (LTD) in Purkinje cells (PCs), leads to hippocampal place cells with unstable fields and impairments in spatial navigation measured as lower escape latencies and worst trajectory optimization than controls in water maze tasks (17, 18). Despite these pieces of evidence that support a role of NU in generating internal estimations of motion and orientation in space, we do not know to what extent PCs in the murine NU encode world-centered (tilt and translation) and/or vestibular afferent-like information (gravito-inertial acceleration or GIA), and

Significance

For spatial navigation, self-centered information sensed by sensory organs is transformed into world-centered information about our motion and orientation in space. The cerebellar posterior vermis helps transform vestibular afferent cues into translation and tilt information, but empirical evidence on the neuronal computations involved is lacking. We investigate these computations using a modeling approach and transgenic mice where protein kinase C (PKC) is inhibited at cerebellar cortex output neurons (Purkinje cells [PCs]). We demonstrate that most PCs have tilt and translation information and that the gain and timing of translation information are modulated by PKC-dependent processes. Hence, translation and tilt information are independently regulated in PCs. Moreover, PKC-dependent processes at PCs participate in generating world-centered motion information.

Author contributions: T.A.Y. and P.M.B. designed research; R.G.H., R.Z., T.A.Y., and P.M.B. performed research; C.I.D.Z. contributed new reagents/analytic tools; R.G.H., R.Z., T.A.Y., and P.M.B. analyzed data; and R.G.H., C.I.D.Z., T.A.Y., and P.M.B. wrote the paper.

The authors declare no competing interest.

This article is a PNAS Direct Submission.

Published under the PNAS license.

Data deposition: The neuronal and stimulus data used for Figs. 1–7 and the data used to run all statistical analysis have been deposited in the GitHub repository, https://github.com/BlazquezPablo/PNAS_2020.

¹To whom correspondence may be addressed. Email: yakushevat@wustl.edu or pablo@wustl.edu.

This article contains supporting information online at <https://www.pnas.org/lookup/suppl/doi:10.1073/pnas.2002177117/-DCSupplemental>.

First published July 7, 2020.

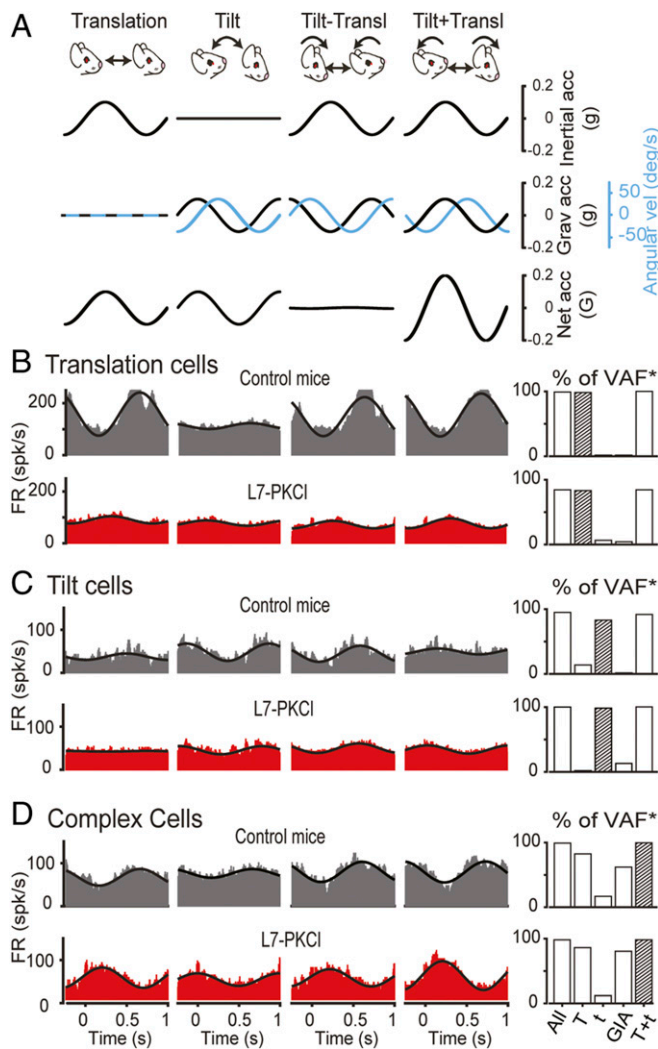


Fig. 1. Response of different types of NU PCs to tilt/translation paradigms in control and L7-PKCI mice. (A) Cartoons illustrating the tilt/translation protocol (Top), and stimuli: inertial acceleration, gravitational acceleration, net acceleration, and angular velocity (blue trace). (B) Example responses of PCs classified as translation-only in the control (Top, gray histograms) and L7-PKCI mouse (Bottom, red histograms). The black traces represent the sinusoidal function that best fitted the neuronal responses. Bar plot at the Right indicates VAF* by different models wherein the best model is indicated by the bar filled with black stripes. Groups in the x axes of the bar plot correspond to the following: All, complex model containing all components; GIA, gravito-inertial model; T, translation model; t, tilt model; T+t, complex model containing tilt and translation components. (C) Same as B, but for PCs classified as tilt-only. (D) Same as B, but for PCs classified as complex.

how molecular pathways like those involved in regulating neuronal plasticity may affect this encoding.

To understand the computations carried out by the NU, we investigated the response of NU PCs in control and L7-PKCI mice to vestibular stimuli designed to selectively activate otolith organs and semicircular canals. By characterizing the differences in PC responses in the normal and L7-PKCI animals, we could unveil neuronal mechanisms responsible for computing translation and tilt information from vestibular afferent signals. Our analyses indicate that NU PC responses can be explained by the presence of translation, tilt, and GIA information. Our findings support the view that NU PCs carry information about our motion and orientation in space and that PKC-dependent mechanisms contribute to shape the response of these neurons during spatial navigation.

Results

We investigated the representation of world-centered and vestibular afferent motion information in NU, and how this representation is modified in L7-PKCI mice (19). These transgenic mice have problems solving spatial navigation tasks when relying exclusively on internal cues (e.g., vestibular information) (17, 18). It has been proposed that these problems originate from a failure of NU in computing world-centered motion information (18, 20). We used a tilt/translation experimental protocol that has proven successful in isolating world-centered (inertial motion, and orientation with respect to gravity) and vestibular afferent (GIA) information in nonhuman primates (15, 21–23) (Fig. 1A). We analyzed the PC simple spike (SS) responses using a computational model that assumes that these responses include both world-centered and vestibular afferent information. By exploiting a PC-specific mouse mutant that has been shown to suffer from solving spatial navigation tasks as well as from abnormalities in postsynaptic plasticity of the parallel fiber (PF) inputs (i.e., the Pf–PC synapse), this computational model allowed us to assess at least part of the essential contributions of PCs in these two forms of information processing.

Representation of Translation, Tilt, and GIA Information in PC Responses.

We recorded the SS responses of NU PCs to our tilt/translation protocol in eight C57BL/6 wild-type mice (CB-wts), nine PKCI wild-type littermates (PKCI-wts), and nine L7-PKCI mice (Fig. 1 and *SI Appendix*, Fig. S1). A total of 104 PCs modulated their response during our tilt/translation protocol ($n = 18$, $n = 37$, and $n = 49$ from CB-wts, PKCI-wts, and L7-PKCI mice, respectively). NU PCs were identified by a pause in SS following complex spikes (CSs) and their characteristic firing properties (20, 21).

Because the firing rate modulation of SS in CB-wts and PKCI-wts was similar, we combined them as controls ($P = 0.435$, $P = 0.849$, $P = 0.08$, $P = 0.140$ comparison for “translation,” “tilt,” “tilt–translation,” and “tilt+translation,” respectively, Mann–Whitney U test). We modeled NU PC responses using a model that assumes that neuronal responses can be explained by the sum of three independent components: a translation component, a tilt component, and a GIA component. Note that a neuron carrying only GIA information would have a strong GIA component, but no tilt or translation component. Using this modeling approach, we were able to explain with high accuracy the responses of 92% of responsive PCs (98/104, %VAF* > 75%). Based on the components that best describe their response to vestibular stimulation, we found four types of PCs: translation-only, tilt-only, GIA-only, and complex PCs.

Translation-only PCs showed responses that correlated with translation motion, while head orientation (tilt) had negligible effect. Two examples of translation-only PCs are shown in Fig. 1B. These cells showed similar modulation during translation, tilt–translation, and tilt+translation paradigms and little or no modulation during tilt. Tilt-only PCs showed responses that correlated well to changes in head orientation with respect to gravity, while translation motion had little or no effect (Fig. 1C). Tilt-only PC responses were best explained by a single tilt input. GIA-only PCs showed responses that are best explained using gravito-inertial information. GIA-only PCs showed little or no modulation during the tilt–translation paradigm. GIA responses resembled the responses of otolith afferents. Translation-only PCs were more abundant than tilt-only and GIA-only PCs in both control (24/53, 1/53, and 0/53, respectively) and L7-PKCI mice (15/45, 3/45, and 2/45, respectively). However, the most abundant PC type was the complex PC (28/53 and 25/45 in control and L7-PKCI animal, respectively), which could be characterized by a combination of two or three response components (Fig. 1D).

The combination of translation and tilt components was overwhelmingly represented in the response of complex PCs (96% [27/28]

and 88% [22/25] in both control and L7-PKCI mice, respectively). In contrast, GIA information (either in combination with translation, tilt, or both) was rarely found in our complex PC population (11% [3/28] and 24% [6/25] for the control and L7-PKCI mouse, respectively). Our data suggest that the translation component is the dominant component in NU PC responses, yet most PCs also contain some tilt information.

Further comparison of control and L7-PKCI data showed that the responses of PCs in control mice were only marginally better explained by our modeling approach than the responses of PCs in L7-PKCI mice (mean \pm SEM of %VAF* was 94.2 ± 0.77 in control mice and 92.1 ± 1.0 in L7-PKCI mice). PCs lacking translation component were rare in controls, while they were somewhat more frequently found in L7-PKCI mice (2% [1/53] control mice, and 13% [6/45] in L7-PKCI mice). Similarly, as mentioned above, we found only 2% (1/53) tilt-only and 0% GIA-only PCs in control mice, while there were 7% (3/45) tilt-only and 4% (2/45) GIA-only PCs in L7-PKCI mice.

Because differences in the percentage of tilt-only and GIA-only neurons in control and L7-PKCI mice could be due to a sampling bias, we next compare data from control and L7-PKCI mice solely in PCs with translation component (i.e., translation-only and complex PCs).

Canal- and Otolith-Related Information in PCs in Control and L7-PKCI Mice. In control mice, PCs with a translation component showed significantly larger firing rate modulation during translation than during tilt (mean \pm SEM; 32.6 ± 2.5 spk/s [$n = 52$] for translation, and 11.7 ± 1.2 spk/s [$n = 49$] for tilt; $P < 0.001$, Wilcoxon signed-rank test; Fig. 2A). Similar results were found in L7-PKCI mice (20.8 ± 1.9 spk/s [$n = 39$] for translation and 13.2 ± 1.4 spk/s [$n = 37$] for tilt; $P = 0.001$, Wilcoxon signed-rank test; Fig. 2A). However, the effect was more pronounced in controls than in L7-PKCI animals (ratio tilt vs. translation modulation was 0.47 ± 0.08 [$n = 49$] in control animals and 0.72 ± 0.12 [$n = 37$] in L7-PKCI mice; $P = 0.013$, Mann-Whitney U test; Fig. 2B). The differential effect resulted from a decrease in PC responsiveness to translation in L7-PKCI animals ($P < 0.001$, $P = 0.302$ for translation and tilt, respectively; Mann-Whitney U test).

Neuronal responses to translation can be used to evaluate signal processing of otolith-related information, while neuronal responses to tilt+translation can be used to evaluate signal processing of semicircular canal-related information (21). Current theories suggest that NU computes world-centered information by combining information from both sensory organs (1, 15). Importantly, this computation requires that the signals from canals and otoliths match at the level of PCs in that these two inputs exert similar effects in both spatial and temporal domain. Our results in mice support this hypothesis in that the gain (amplitude) and phase (timing) of the PC responses are similar for both sensory inputs.

PC response amplitudes to translation were not different from those to tilt+translation, in neither controls nor L7-PKCI animals ($P = 0.249$ and $P = 0.081$, respectively, Wilcoxon signed-rank test; Fig. 2C). Comparison on a cell-by-cell basis further validated our findings. The ratios of the amplitude of modulation during tilt+translation vs. translation were near 1 in controls and L7-PKCI animals (1.1 ± 0.07 [$n = 52$] and 0.97 ± 0.13 [$n = 34$], respectively; Fig. 2D). The response during translation was also not significantly different from the response during tilt+translation for controls and L7-PKCI mice ($P = 0.202$ and $P = 0.052$, respectively, Wilcoxon signed-rank test; SI Appendix, Fig. S2A). Moreover, the response amplitude ratio during translation vs. tilt+translation was near unity for both types of mice ($P = 0.615$, Mann-Whitney U test; SI Appendix, Fig. S2B).

In control animals, the PC response phase during translation was not significantly different from that during tilt+translation (normalized responses between $\pm 90^\circ$ [deg]: $30.8^\circ \pm 3.5^\circ$ [$n = 52$]

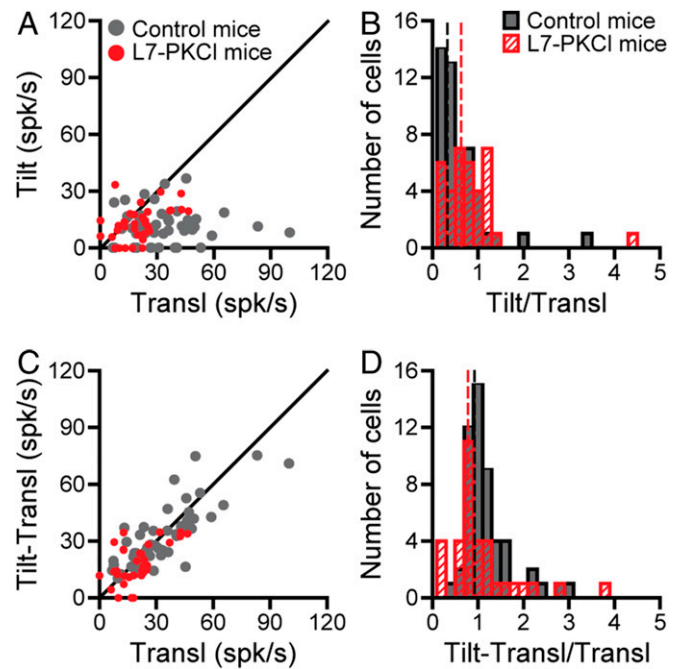


Fig. 2. PCs in both control and L7-PKCI mice showed similar canal- and otolith-related information, although L7-PKCI mice show smaller responses to translation. (A) XY plot showing the response amplitude (in spikes per second) during translation vs. tilt paradigms. The gray and red data points correspond to control and L7-PKCI PCs, respectively. (B) Histogram showing the amplitude response ratio for tilt vs. translation. The gray and red bars correspond to control and L7-PKCI PCs, respectively (mean \pm SEM; 0.47 ± 0.08 in control and 0.72 ± 0.12 in L7-PKCI mice; $P = 0.013$, Mann-Whitney U test). Median values are shown as vertical dashed lines. (C) Same as A, but for translation vs. tilt+translation paradigms. (D) Same as B, but for the ratio tilt+translation vs. translation (1.1 ± 0.07 in control and 0.97 ± 0.13 in L7-PKCI mice; $P = 0.046$, Mann-Whitney U test).

vs. $29.2^\circ \pm 4.4^\circ$ [$n = 52$], respectively, $P = 0.647$, Mann-Whitney U test; Fig. 3A, gray histograms). This similarity was also true when comparing the phases on a cell-by-cell basis ($P = 0.217$, Wilcoxon signed-rank test; Fig. 3B, gray data points and histograms). We obtained qualitatively similar results in L7-PKCI mice. Response phases during translation and tilt+translation in L7-PKCI mice were not different at the population level ($-2.5^\circ \pm 5.7^\circ$ [$n = 37$] vs. $11.9^\circ \pm 6.8^\circ$ [$n = 36$]; $P = 0.180$, Mann-Whitney U test; Fig. 3A, red histograms) or cell by cell basis ($P = 0.617$, Wilcoxon signed-rank test; Fig. 3B, red data points and histograms). However, there was a notable difference between control and L7-PKCI mice in that the responses to translation and tilt+translation in the L7-PKCI mice lead those found in the controls by about 25° ($P < 0.001$ and $P = 0.003$, respectively, Mann-Whitney U test; Fig. 3A).

Our data indicate that for both control and L7-PKCI mice gain and phase during translation and tilt+translation are matched in each PC, suggesting that signals originated in semicircular canals and otoliths matched adequately. This is an essential computational step to compute world-centered information. Remarkably, at the population level, L7-PKCI PC responses to translation and tilt+translation showed smaller gain and phase than controls.

Translation and Tilt Components in PC Responses in Control and L7-PKCI Mice. Next, we investigated how translation and tilt components were represented in the response of NU PCs. Because of the low number of tilt-only and GIA-only PCs, component comparisons were only valid for translation-only and complex PCs. Specifically, we tested 1) whether the translation component in

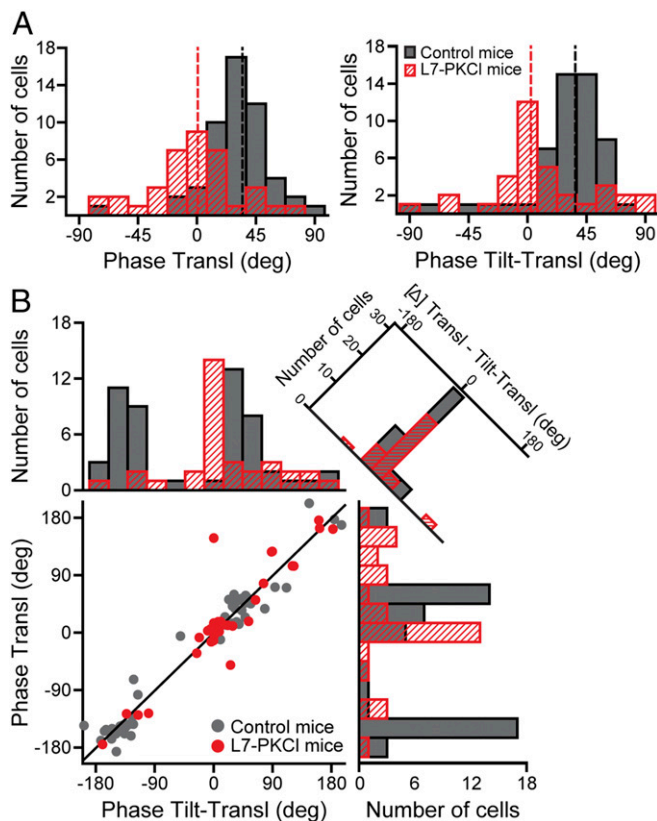


Fig. 3. Temporal information (phase) is matched in PC in control and L7-PKCI mice, but PC response phase in L7-PKCI lead those in control mice. (A, Left) Response phases to translation paradigm normalized to $\pm 90^\circ$ for control and L7-PKCI mice (gray and red histograms, respectively; mean \pm SEM; 30.8 ± 3.5 [$n = 52$], and -2.5 ± 5.7 [$n = 37$], $P < 0.001$ Mann-Whitney U test). (Right) Same as Left but for tilt-translation paradigm (gray and red histograms, respectively; 29.2 ± 4.4 [$n = 52$], and 11.9 ± 6.9 [$n = 36$], $P = 0.003$ Mann-Whitney U test). Median values are shown as vertical dashed lines. (B) Cell-by-cell comparison of phases during translation vs. tilt-translation (bottom-left plot and top-right histogram), and population data from -180° to 180° (top-left and bottom-right histograms). The difference in the PC response phase to translation and tilt-translation approximate zero in control and L7-PKCI mice (-1.9 ± 3.1 and 4.9 ± 7.3 [$n = 35$], respectively; $P = 0.463$ Mann-Whitney U test).

translation-only and complex cells share the same characteristics, and 2) whether translation and tilt components are affected in L7-PKCI mice. In these analyses, the translation component corresponded to that obtained from the model fitting (*Experimental Procedures, Description of Computational Models*).

The amplitude and phase of the translation component were similar for translation-only and complex PCs in control as well as L7-PKCI mice ($P = 0.554$ [amplitude] and $P = 0.190$ [phase] for control animal, and $P = 0.698$ [amplitude] and $P = 0.386$ [phase] for L7-PKCI animal, Mann-Whitney U test; gray and red histograms in Fig. 4A, Top in Fig. 4B). These findings indicate that translation-only and complex PCs share the same translation information.

Interestingly, PCs in control mice showed larger translation components than PCs in L7-PKCI mice ($P = 0.008$ and $P = 0.023$ for translation-only and complex PCs, respectively, Mann-Whitney U test; gray vs. red histograms in Fig. 4A, Left, and Fig. 4B, Top Left), but a similar tilt components ($P = 0.415$, Mann-Whitney U test; gray vs. red histograms in Fig. 4B, Bottom Left). Comparison of the phase of the tilt and translation components in control and L7-PKCI mice showed mixed results. There were no differences in

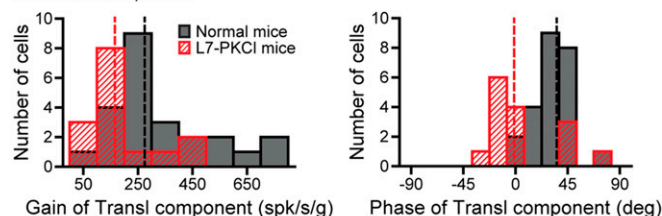
the phase of the translation and tilt components in complex PCs ($P = 0.183$ and $P = 0.791$, respectively, Mann-Whitney U test; gray vs. red histograms from Fig. 4B, Right), but translation-only PCs showed different phases in control and L7-PKCI mice ($P = 0.007$, Mann-Whitney U test; gray vs. red histograms in Fig. 4A, Right). These results suggest that the gain of the translation component is the main element affected in L7-PKCI animals.

Spatial Tuning in Control and L7-PKCI Mice. Next, we examined the responses of NU PCs during translation and tilt-translation paradigms along different directions to calculate the directional tuning of otolith- and canal-driven information in PCs (for translation-only and complex cells, $n = 25$ in control and $n = 17$ in L7-PKCI animals). We calculated the preferred directions and tuning ratios of neuronal responses along different azimuths (as in ref. 22) (Fig. 5 and *SI Appendix, Fig. S3*).

In control animals, the preferred directions for translation and tilt-translation were distributed throughout the entire range of azimuth directions (Fig. 5A, gray data). Within-cell comparisons indicated that most cells showed the same preferred direction for translation and tilt-translation ($P = 0.742$, Wilcoxon signed-rank test; Fig. 5A, gray bars in top right histogram). The average tuning ratio, measured as the ratio between the minimum and maximum response, was similar for translation and tilt-translation (0.22 ± 0.04 and 0.22 ± 0.04 , respectively, $P = 0.943$,

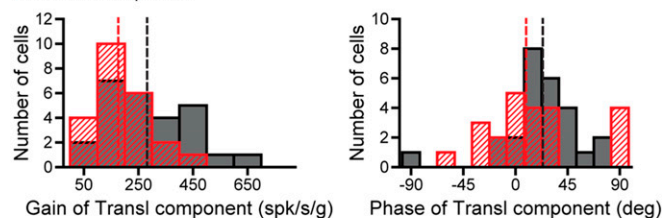
A Translation only cells

Translation component



B Complex cells

Translation component



Tilt component

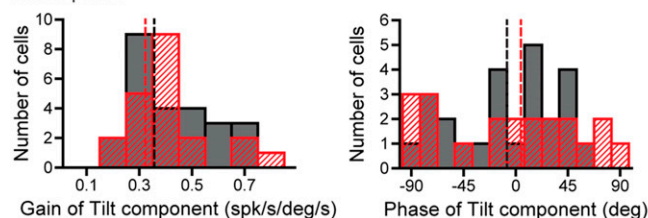


Fig. 4. Gain and phase of translation and tilt components in PC responses reveal that the translation component is altered in L7-PKCI mice. (A) Comparison of gains (Left) and phases (Right) of the translation component in translation-only PCs between control and L7-PKCI mice ($P = 0.008$ and $P = 0.007$, respectively, Mann-Whitney U test). (B, Top) Same as A for the translation component of complex PCs ($P = 0.023$ [gain] and $P = 0.183$ [phase], Mann-Whitney U test). (B, Bottom) Same as A for the tilt component of complex PCs ($P = 0.415$ [gain] and $P = 0.791$ [phase], Mann-Whitney U test). The gray and red bars represent control and L7-PKCI data, respectively. Median values are shown as vertical dashed lines.

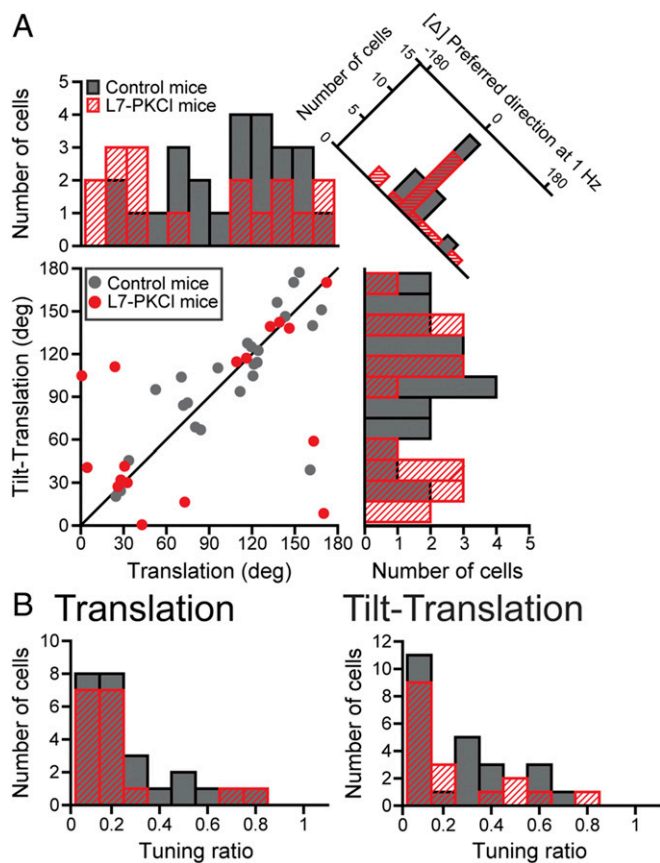


Fig. 5. PCs in control and L7-PKCI mice had the same preferred direction for canal- and otolith-driven information. (A) Histograms showing the distribution of PC preferred azimuth directions for translation (Top Left) and tilt-translation (Bottom Right). (Bottom Left) X/Y plot of preferred azimuth for translation and tilt-translation of individual PCs. (Top Right) Difference between preferred direction to translation and tilt-translation of individual PCs ($P = 0.742$, Wilcoxon signed-rank test). (B, Left) Spatial tuning ratio for translation calculated as the ratio between the minimum and maximum response. (B, Right) Same as Left but for tilt-translation. The method used to calculate the preferred azimuth is illustrated in *SI Appendix, Fig. S2*.

Wilcoxon signed-rank test; Fig. 5B, gray data). This indicates not only that translation and tilt-translation preferred directions are spatially well aligned, but also that they are quantitatively equally well tuned to the preferred direction.

The response of PCs in L7-PKCI mice showed similar spatial tuning characteristics as in control mice. The preferred azimuth directions for translation and tilt-translation in L7-PKCI mice were widely distributed (Fig. 5A, red data). Individual L7-PKCI PCs showed similar preferred directions to translation and tilt-translation ($P = 0.927$, Wilcoxon signed-rank test; Fig. 5A, red bars in top right histogram). Likewise, the tuning ratio was similar for translation and tilt-translation (0.18 ± 0.05 and 0.20 ± 0.05 , respectively, $P = 0.747$, Wilcoxon signed-rank test; Fig. 5B, red data).

Overall, our data indicate that canal and otolith information are matched spatially at the individual PC level. In contrast to the data obtained in macaques (15), we found no preference for azimuth directions at the population level. These findings were true for control and L7-PKCI mice.

Dynamic Response Properties. We examined whether the gain and phase of NU PC responses change with frequency to elucidate to what extent these neurons carry motion information other than

inertial acceleration. In line with Yakusheva et al. (24), we anticipated that decreases in neuronal gain (spikes per second per g) and increases in neuronal phase with frequency would suggest that neurons carry signals related to slower components (i.e., inertial velocity), while the opposite would indicate that they carry faster components (i.e., jerk).

PC response gains to translation and tilt-translation slightly increased with frequency up to 1 Hz in both control and L7-PKCI mice (Fig. 6A, Top). These results stand in marked contrast to those obtained in macaques, where neuronal gain significantly decreases with frequency (24). Remarkably, gains were smaller in L7-PKCI mice than control animals for most tested frequencies ($P < 0.014$, Mann-Whitney U test; Fig. 6A, Bottom).

NU PC response phases to translation and tilt-translation decreased with frequency in control and L7-PKCI mice ($P < 0.008$ and $P < 0.008$ for translation and tilt-translation, respectively, Wilcoxon signed-rank test; Fig. 6B, Top). In control animals, peak firing rate lagged acceleration at 0.18 Hz by more than 90° (mean \pm SEM; $91.5^\circ \pm 8.7^\circ$ [$n = 7$] and $126.8^\circ \pm 2.7^\circ$ [$n = 3$] for translation and tilt-translation, respectively), while it led acceleration by more than 20° at 2 Hz ($-20.6^\circ \pm 7.6^\circ$ [$n = 14$] and $-45.3^\circ \pm 13.7^\circ$ [$n = 13$] for translation and tilt-translation, respectively; Fig. 6B, Bottom). These response dynamics differ from those observed in macaques, where phases do not show a clear change with frequency (24).

Our data suggest that NU PCs in wild-type mice carry mostly acceleration information because their gain is unaffected by frequency. The observed changes in phase with frequency may indicate jerk signals; however, the marginal increase in gain with frequency suggests that jerk signals have, at most, a minor influence on PC responses. Because the phase differences observed between control and L7-PKCI mice for 1 Hz are maintained throughout the entire range of frequencies tested, the general dynamic response properties of NU PCs appear to be relatively unaffected in L7-PKCI mice.

CS Responses to Tilt/Translation Paradigms. We analyzed the CS responses of 19 PCs from control and L7-PKCI mice along the preferred azimuth direction of their SSs. These PCs were classified as translation and complex cells based on their SS responses (five for control and one for L7-PKCI mice, and four for control and nine for L7-PKCI mice, respectively). All these PCs showed significant CS and SS responses to our tilt/translation paradigms. The phase relationship between CSs and SSs was more broadly distributed in control than L7-PKCI mice for all paradigms (SD of 108.3 and 30.3, respectively; Fig. 7A).

We investigated whether CSs and SSs carry similar information by comparing the response amplitude of CSs and SSs to our tilt/translation paradigms. If CSs would carry the same information as SSs, we would expect that CS responses would be predicted by SS responses in each PC. For instance, PCs showing half the SS response to tilt than to translation would also show half the CS response to tilt than to translation. Interestingly, this was neither the case for the control nor the L7-PKCI mice. Namely, CS responses were characterized by having strong responses to tilt, even when the SS response to tilt was weak (Fig. 7B and *SI Appendix, Fig. S4*). When normalizing CS and SS responses with respect to their response to translation, we observed that SS responses did not predict CS responses in the same PC (median slope = -0.28 , and -0.03 for control and L7-PKCI mice, respectively, and median $r^2 = 0.23$, and 0.04 for control and L7-PKCI mice, respectively; *SI Appendix, Fig. S5*). CS responses in control and L7-PKCI mice were not significantly different (amplitude of modulation during each paradigm, $P > 0.230$, Mann-Whitney U test).

CS response phases to translation and tilt-translation paradigms were similar in control and L7-PKCI mice, albeit a larger spread of phases in the control animal ($P > 0.185$, Mann-Whitney

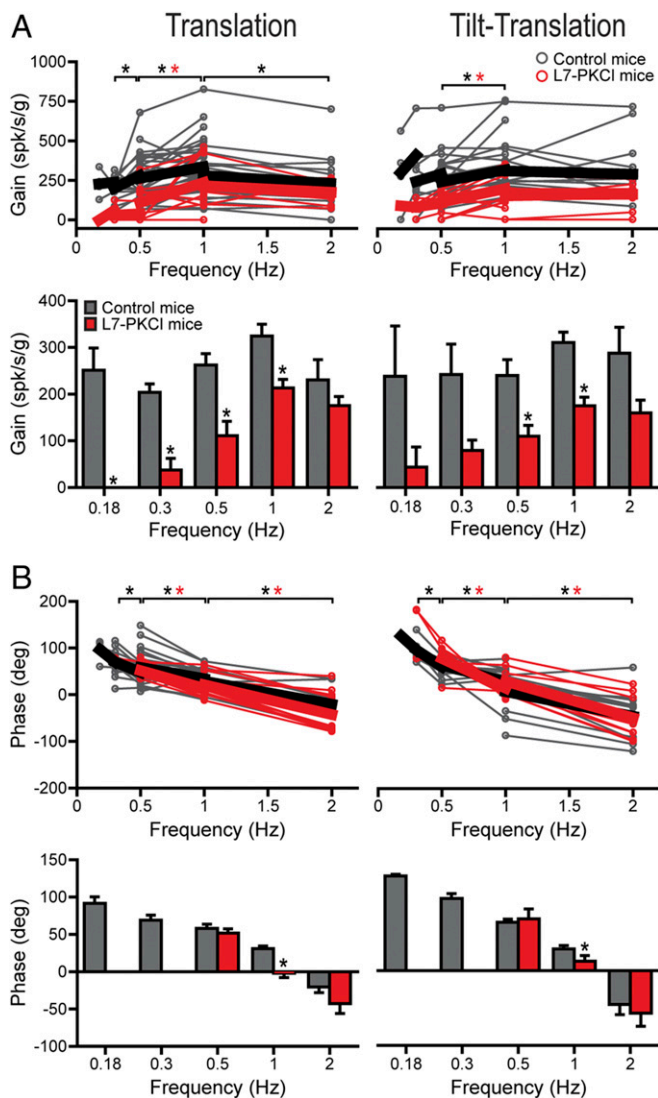


Fig. 6. Neuronal gain and phase to translation and tilt-translation paradigms changed with frequency in control and L7-PKCI mice. (A, *Top*) Neuronal gain of individual cells (dots connected by thin lines) to translation and tilt-translation underwent small increases with frequency, peaking at 1 Hz in control and L7-PKCI mice (gray and red symbols, respectively). Only neurons recorded during at least two consecutive frequencies were included in the *Top*. Thick lines represent the evolution of the gain of the average response. (A, *Bottom*) Histograms showing marginal increases in the population gain to translation and tilt-translation, respectively, with frequency in control and L7-PKCI mice. The gain to translation and tilt-translation in L7-PKCI was smaller than control animal ($P < 0.014$, Mann-Whitney U test). Stars indicate a $P < 0.05$ level of statistical significance (Wilcoxon signed-rank test [*Top*] or Mann-Whitney U test [*Bottom*]). (B) Same than A but for neuronal phase. (*Top*) Response phase of individual PCs to translation decreases with frequency in control and L7-PKCI mice ($P < 0.008$, Wilcoxon signed-rank test). (*Bottom*) Histograms show that the neuronal phase of the population of control and L7-PKCI PCs to translation and tilt-translation decreases with frequency.

U test; Fig. 7C). It can be also appreciated that, when normalized to $\pm 90^\circ$, CS phases fell closer to 0° in L7-PKCI mice than control mice (resembling the SS data shown in Fig. 3A and B); thus, suggesting that CSs in L7-PKCI animals have slightly more acceleration signals than in normal animals.

Overall, our data suggest that CS responses do not mirror SS responses, that CSs carry combined tilt and translation information, that tilt information is proportionally larger in CS

than SS responses, and that CS responses are generally unaffected in L7-PKCI animals.

Discussion

We investigated how inertial acceleration (translation) and head orientation with respect to gravity (tilt) are represented in the responses of NU PCs in control mice and mutants that overexpress an inhibitor of PKC specifically in their PCs (L7-PKCI mice; ref. 19). We found that canal and otolith information are matched spatially and temporally at the level of PCs in both control and L7-PKCI mice. We developed a computational model that explains NU PC SS responses through a combination of tilt, translation, and GIA information. We found that most PCs in control and L7-PKCI mice carry tilt and translation information and that the translation component is identical in translation-only and complex PCs. Importantly, control and L7-PKCI PCs carry different translation information, both in magnitude and phase, but similar tilt information. In contrast to SS, CS responses are largely unaffected in L7-PKCI mice. These results suggest that the NU is well designed to generate world-centered (e.g., translation and tilt) information from vestibular

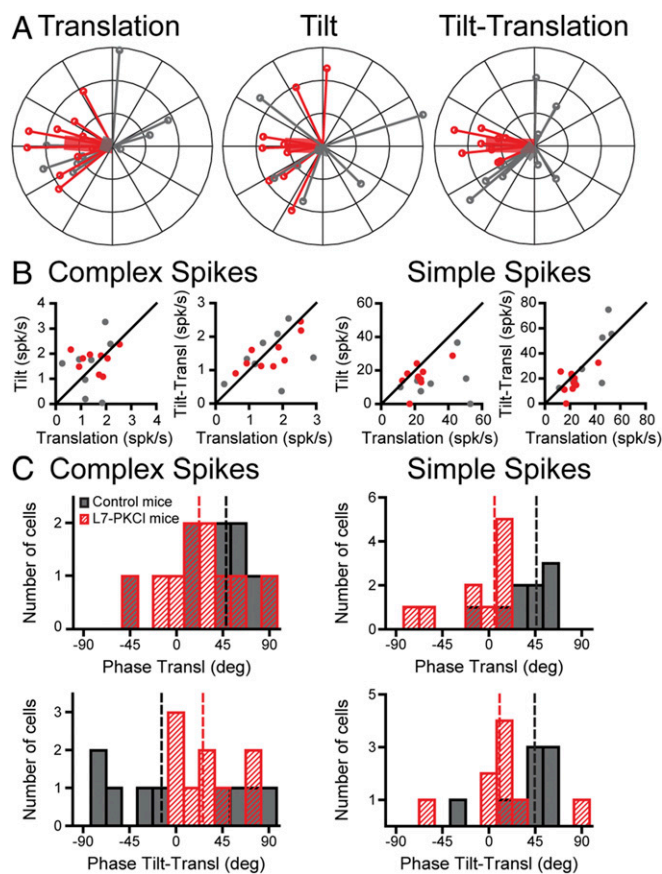


Fig. 7. CS responses do not mirror SS responses and are unaffected in L7-PKCI mice. (A) Polar plots showing the phase of CS with respect to SS (vector direction) and amplitude of modulation of CS (vector size) during translation (*Left*), tilt (*Center*), and tilt-translation (*Right*). Control and L7-PKCI data are represented in gray and red, respectively. *SI Appendix, Fig. S3* shows examples of simultaneous CS and SS recordings. (B) XY plots showing the response amplitude of CS (two *Left* panels) and SS (two *Right* panels) during translation vs. tilt, and translation vs. tilt-translation paradigms. The diagonal is represented as a solid black line. (C) Normalized phase of CS and SS (*Left* and *Right*, respectively) to $\pm 90^\circ$ during translation and tilt-translation paradigms (*Top* and *Bottom*, respectively). Median values are represented with vertical dashed lines. Examples of how this normalization is performed are shown in *SI Appendix, Fig. S4*.

afferent-like (e.g., otolithic and canal afferents) signals and that it engages PC-specific mechanisms to compute these signals.

Implications of Our Modeling Approach. We and others have proposed that NU PC responses carry translation, tilt, and/or GIA information (1, 16, 21) and that translation information is computed by subtracting tilt position information, originating in the semicircular canals, from GIA information, originating in the otolith organs. This concept is supported by the impact of canal plugging, which results in loss of world-centered information in NU PCs and emergence of responses that resemble those of otolith afferents (4, 15). Mathematically, to compute pure translation information from tilt and GIA information, there must be a perfect match between the amount of tilt and GIA information (5, 6). However, because biological systems are intrinsically noisy, residual tilt or GIA signals are likely present after computing translation at these computational nodes. Therefore, our modeling approach, which considers the existence of complex cells, may represent natural data more realistically.

We found that most NU PCs carry tilt and translation information while few carry GIA information. One interpretation of this finding is that there is more tilt than GIA information at the computational node where tilt and GIA information are combined to generate translation information. In support of the dominance of tilt and translation signals in PCs, macaque NU PCs have been classified as either translation or tilt (1, 16) and most NU PCs in mice are responsive to static tilt (80% in ref. 25). Interestingly, the large number of complex cells in our dataset suggest that complete separation of tilt and translation, if it occurs, happens downstream of NU PCs.

Spatial and Temporal Alignment of Canal- and Otolith-Related Information Is Intact in L7-PKCI Mice. Before canal- and otolith-related information are combined to generate an estimation of translation, they must be aligned spatially (preferred direction) and temporally (phase for sinusoidal stimuli) (1, 6). In line with this concept, our data in control and L7-PKCI mice showed that the preferred direction for translation when only otolith organs are stimulated (translation paradigm) aligns with the preferred direction for translation when only semicircular canals are stimulated (tilt–translation paradigm). Similarly, the response phases to translation motion when only otolith organs are stimulated match those to translation motion when only canals are stimulated over the entire range of frequencies tested (0.18 to 2 Hz). Together with previous data obtained in macaques (15), our data suggest that rodents and primates use the same general computations to generate world-centered information and that cellular mechanisms dependent on the activity of PKC in PCs, such as postsynaptic LTD at Pf–PC, are not required per se in the spatiotemporal alignment of information of canal and otolith origin.

The spatiotemporal alignment of canal- and otolith-related information in NU PCs in L7-PKCI mice suggests that this alignment is done upstream of NU PCs, for example by the circuit formed by cerebellar cortical interneurons. This circuit is well suited to perform these computations (26, 27). For instance, molecular layer interneurons can perform signal integration, gain modulation, and timing- and context-dependent processing (27–32), and thereby control the gain and timing of cerebellar PCs (27, 33–36). Likewise, type I unipolar brush cells, an abundant class of interneurons in the vestibulocerebellum (37–39), can show a spatial preferred direction that is opposite to that of their mossy fiber inputs (40, 41). An alternative interpretation is that, within the same cell type, e.g., PCs, mechanisms independent of PKC in PCs participate in computing estimations of tilt and translation. For instance, enhancing the synaptic weight of Pf–PC synapses through induction of long-term potentiation (LTP) may also be involved in generating accurate estimations of our motion and orientation in space. This concept is supported

for example by the presence of unstable hippocampal place fields in mouse lacking LTP induction at their Pf–PC synapses (42).

NU PC responses to translation and tilt–translation in control and L7-PKCI mice lag and lead head acceleration at low and high frequencies, respectively. A comparable change was noted in wild-type anesthetized mice during sinusoidal tilt (25). Interestingly, L7-PKCI PCs showed responses that generally lead those of control animals throughout the tested frequency range. This phase lead indicates impairments in the regulation of SS timing in L7-PKCI PCs. In support, LTD at Pf–PC has been shown to contribute to changes in the timing of PCs and related behavioral responses (43). During eyeblink conditioning, LTD operates synergistically with the molecular layer interneurons to induce a suppression in SS responses that elicits the timing-dependent conditioned response (27, 44). Our data also showed small gain increases to otolith- and canal-related information with frequency, which together with the increase in phase lead with frequency suggest that mouse NU PCs carry more acceleration signals than those in macaques (24). Similar differences have been observed between mammals with lower and higher body weights in the dominant frequency of their eyelid responses (45).

CSs in Control and L7-PKCI Mice Show Similar Response Properties. Like SSs, CSs responded to translation and tilt. However, CS responses have larger tilt vs. translation information than their SS counterparts. Our results agree with previous studies showing that SS modulations in the vestibulocerebellum do not always follow CSs in a reciprocal fashion as canonically portrayed (26, 46–50). For instance, the spatiotemporal properties of CSs do not reciprocate those of SSs in macaque NU (51) and CSs can modulate during vestibulo-ocular reflex (VOR) in the dark when SS responses are largely absent or in-phase with CS responses (49). Comparison of control and L7-PKCI mice indicates that PKC-dependent processes has only a marginal effect on the climbing fiber response. Similarly, CS responses in the mouse flocculus of L7-PKCI animals appear normal (52).

Formation of Translation-Related Information in PCs Depends on PKC. The translation component was the only component affected in the SS responses of L7-PKCI PCs. Consequently, L7-PKCI PCs showed smaller SS modulations to translation than control PCs, but comparable SS responses to tilt. This finding indicates that PKC-dependent processes in PCs modulate the translation component, but not the tilt component, highlighting that translation and tilt information are delivered to NU PCs via two independently regulated pathways.

The diagram shown in Fig. 8 depicts a functional interpretation of our results. Tilt and translation signals must be computed, at least partly, upstream of the Pf–PC synapse and must arrive at PC via two separated information pathways, because only the translation component appears affected in L7-PKCI mice. This interpretation is further supported by the finding that the otolith- and canal-related translational component in L7-PKCI PCs are spatially and temporally aligned, which is a key requirement to compute translation. We argue that PKC-dependent processes in PCs may contribute by modifying the gain of the pathway carrying translation information and by shifting the phase (timing) of the translation signal. Both adjustments in the translation component may be crucial for downstream computations, such as those carried out by fastigial neurons. Specifically, it has been hypothesized that fastigial neurons compare the predictions generated by the cerebellar cortex (i.e., forward model) with the sensory consequences of those predictions. The error or sensory prediction error generated through this comparison is used to modify the forward model (53–59). For this relatively simple comparator network to work, the gain and phase of the prediction must match those of the sensory consequences. We hypothesize that this delicate balance is perturbed in L7-PKCI

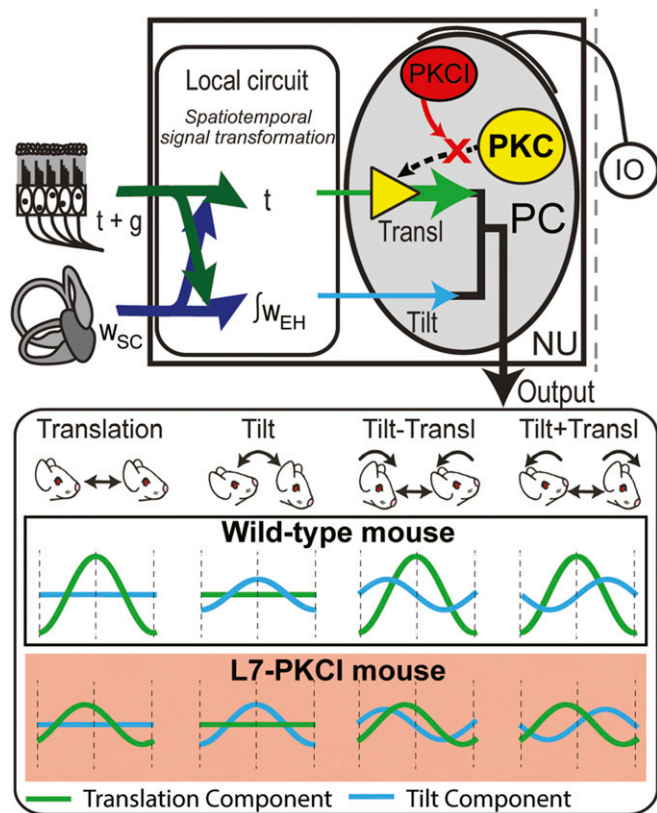


Fig. 8. Schematic representation of the proposed computations carried out by NU. (Top) Schematic showing the information flow. Semicircular canal afferents respond to angular head motion (ω) in head-centered reference frame. Otolith afferents encode GIA. The CNS transforms vestibular afferent information into world-centered information (tilt [ω_{EH}] and translation [t]). Because NU PCs in L7-PKCI animals show good spatiotemporal match of canal and otolith signals, we propose that this match is done upstream of PCs. We hypothesize that PKC-dependent processes in PCs modulate the gain and timing of pathways carrying translation information to PCs because only the translation component is affected in L7-PKCI PCs. At the Bottom of the figure, we show the output of this network, represented as PC firing rate modulation during our tilt/translation paradigms. In comparison to wild-type mice, the translation component (green trace) in the L7PKCI mice is smaller and with a phase shift. The tilt component (blue trace) does not change. Abbreviations: g, gravitational acceleration; IO, inferior olive; NU, nodulus and uvula; PC, Purkinje cell; PKC, protein kinase C; t, translation; ω_{EH} , angular head rotation along the earth horizontal axis (tilt); ω_{SC} , angular head motion in semicircular canal coordinates.

mice and that the resulting aberrant signal is responsible for the navigation problems found in these mice (17). Alternatively, the mammalian brain navigation system may be set to work with large translation signals in that the small translation component found in L7-PKCI mice does not provide enough certainty on motion direction, thus leading to unstable place fields and under-performance in water maze tasks (17, 18).

Candidate PKC-Dependent Processes Responsible for the Observed Changes in L7-PKCI Mice. A strength of the L7-PKCI mouse model to understand cerebellar function is that the expression of the inhibitor of PKC in the cerebellum is unique to PCs; thus, the affected mechanisms are PC specific. Gross motor function in L7-PKCI mice appears normal as indicated by the lack of ataxia and normal performance in the rotarod and thin rod tasks (19). Baseline oculomotor performance is also unaffected during VOR and optokinetic reflex (56). Behavioral impairments in L7-

PKCI mice narrow down to deficits on motor learning tasks such as VOR learning and eyeblink conditioning (19, 60, 61). Indeed, the only described physiological deficit in L7-PKCI PCs is the blockage of LTD induction, whereas LTP induction appears intact (19). Therefore, lack of postsynaptic LTD is one of the potential mechanisms responsible for the differential response of posterior vermis PCs between the normal and L7-PKCI mice.

PC morphology and firing properties appear normal in young adult L7-PKCI mice (52, 62); however, a larger fraction of L7-PKCI PCs (47% in L7-PKCI vs. <10% in wild-type mice) are innervated by two climbing fibers (19). This double innervation has only a nominal effect in SS and CS modulation as indicated by the lack of detectable effects on SS and CS responses in the cerebellar vermis, paramedian lobe, and flocculus of L7-PKCI mice (52, 62). Double innervation may affect normal climbing fiber-dependent synaptic plasticity, particularly if the two climbing fibers carry different information. However, since climbing fiber innervation is organized in functional zones, it is likely that a pair of climbing fibers innervating a single PC contains similar information (63, 64). This could explain why CS responses in the flocculus of L7-PKCI mice are indistinguishable from those of normal animals (52).

As PCs in L7-PKCI mice overexpress the inhibitor of PKC in the cytoplasm, LTD induction is probably disrupted at all of its Pf inputs (19). Therefore, we argue that LTD might play a role in modulating translation information in PCs. However, we cannot exclude that PKC also exerts other effects in the cytoplasm of PCs and hence biases our interpretation. One might argue that there are also alternative experimental ways to manipulate LTD induction, for example by altering amino acids of the GluR2 AMPA subunit, which is mainly expressed at the level of the synaptic membrane, thereby possibly eliminating main side effects in the cytoplasm (65). Likewise, one may nowadays affect LTD expression through optogenetic means (66). However, with these approaches too, there may well be other specific or compensatory effects, which are hard to circumvent (44).

Conclusions

Our data in control and L7-PKCI mice provide important insights into the neuronal computations that generate world-centered information from vestibular afferent information in NU. First, canal- and otolith-related information are matched spatially and temporally before reaching PCs. Second, translation and tilt information likely arrive at PCs precomputed in separate information pathways. Third, PKC-dependent processes specifically in PCs may modulate the gain of the information pathway carrying translation information. We hypothesize that the spatial navigation problems and instability of hippocampal place cells observed in L7-PKCI mice are the result of aberrant translation signals in NU PCs that are subject to altered levels of synaptic plasticity.

Experimental Procedures

Animal Preparation. Data were collected from 26 mice of 5 to 16 mo of age. Eight animals were C57BL/6 wild-type, nine were L7-PKCI, and nine were littermate. We used standard methods to prepare animals for recordings (SI Appendix, Methods). In brief, we implanted a plastic recording chamber and head-plate tilted 25° to 30° under isoflurane anesthesia (1 to 2%). All animals underwent a minimum postsurgical recovery period of 3 d before experiments begin. Neuronal recordings were performed without anesthesia. Animals remained calm and awake during recording sessions. Each mouse was subjected to three to seven recording sessions of 3 to 4 h separated by 1 to 3 d of rest.

Surgical and experimental protocols were in accordance with the NIH guidelines and approved by the Washington University Committee on Animal Care. Mice were euthanized with euthasol (50 mg/kg) at the end of their experimental life.

Experimental Setup. Experiments were performed in our vestibular testing system (VTS). The VTS consists of two motorized gimbals mounted on top of a sled. The sled provides linear displacement of up to 1 m. One of the motorized gimbals controls rotations around the earth vertical axes, which corresponds to yaw in our system. The second motorized gimbal controls rotations around the earth horizontal axes. Also, a manually controlled gimbal allows the experimenter to change the azimuth orientation of the animal between +45° to -45°. We considered zero azimuth head orientation to a head orientation aligned with the direction of forward motion of the sled. The azimuth head orientation takes positive and negative values for head orientations to the right and left of the zero azimuth (from the mouse point of view), respectively. Mice had their heads fixed to the VST during recordings through their head-plate such that the center of the head coincided in the center of rotation of the VTS.

A PC desktop computer, Spike2 software, and a Power 1401 system (Cambridge Electronic Design) were used to capture and deliver the vestibular stimuli: sled translational acceleration, Earth vertical rotational velocity, and Earth horizontal rotational velocity (captured at 200 Hz).

Neuronal Recordings and Tissue Preparation. Neuronal activity was amplified by a NB-100 recording system using metal electrodes (FHC; 2- to 6-M Ω impedance). Electrodes were advanced into the tissue using a Servo 2000 microdriver system (National Aperture). Raw neuronal data (40 kHz) were acquired using a PC computer, Spike2 software, and a Power 1401 system. NU PCs were identified by the presence of CSs and SSs. When possible, we identified PCs by the presence of a pause in their SSs following each CS. Alternatively, we used the method described by Hensbroek et al. (67) to verify that the firing properties of the recorded unit are those of PCs. We obtained fewer clean CS recordings than SS recordings because during our recordings we focused mainly on maintaining good isolation of SSs. We did not include CSs from PCs where CSs could only be sporadically isolated because of worries of generating many false negatives. Most of our CS data were recorded during vestibular stimulation at 1 Hz and at the preferred azimuth direction of SS because that was the first paradigm that we fully tested in each PC. The location of each electrode track was mapped with respect to the most anterior part of the chamber using an imaginary grid of 0.25-mm squares. Electrolytic lesions were made in the last recording session in six mice (four control, and two L7-PKCI). Following, the animal was euthanized (50 mg/kg of euthasol) and perfused with saline and fixative (2% PFA in 0.1 M PBS, pH 7.4), and the brain tissue removed and cut in longitudinal sections (40 μ m) to identify the site of the lesion.

The neurons presented in this study were recorded within 0.75 mm of the midline in lobule X and the ventral portion of lobule IX of the cerebellar vermis (nodulus and ventral uvula, respectively). To confirm the recording location as NU, we performed histological reconstruction of the recording locations using the electrolytic lesion as a landmark. A map of the lesions confirming the recording location as being in NU is shown in *SI Appendix, Fig. S1*.

Experimental Protocol. Our vestibular stimuli consisted of sinusoidal stimulation in darkness. We used the tilt/translation experimental protocol previously employed in macaques (Fig. 1A and *SI Appendix, Fig. S1*). This protocol was designed to test whether neurons discriminate tilt from translation. The tilt/translation protocol consists of four vestibular paradigms: translation, tilt, tilt-translation, and tilt+translation. Translation and tilt motions were matched in amplitude and phase such that during tilt-translation the net linear acceleration was zero, and during tilt+translation the net linear acceleration was twice that observed during translation. Stimuli were delivered at 0.18, 0.3, 0.5, 1, and 2 Hz. We used 0.1 g of translation stimulation for all frequencies except for 0.18 Hz, where we used 0.068 g (the sled system maximum travel is 125 cm). We calibrated our tilt stimuli for each frequency using an accelerometer such that it generated the same *g* force as the corresponding translational stimulus for that frequency (e.g., 36.5 deg/s peak velocity of tilt stimulation at 1 Hz). To verify that mice were receiving the desired vestibular stimulation, in some recording sessions, we delivered our vestibular stimulation paradigms while recording data from a three-dimensional (3D) linear accelerometer (NeuwGhent Technology) mounted where the head of the animals was placed.

To investigate the two-dimensional (2D) tuning of PCs, we compared responses to motion in the naso-occipital direction (0 azimuth direction) to responses to motion +45° and -45° azimuth away from the naso-occipital direction (15) and use a cosine curve fit to estimate the preferred azimuth, which corresponds to the azimuth orientation that generates the largest response. We used 1-Hz stimulation to investigate the 2D tuning because,

during our initial recordings, we observed that PCs responded more strongly to 1-Hz vestibular stimulation.

Data Analysis and Cell Classification. Data analysis was carried out in Matlab 2018a (Mathworks) using custom-made programs. Neuronal responses were first averaged over cycles generating a peristimulus-time histogram (PSTH) of 0.005-ms bin size with seven-point moving average for SSs, and 0.1 bin size for CSs. PSTHs were fitted with a sine function to obtain neuronal response phase (in degrees) and amplitude (in spikes per second). PCs were considered responsive to any given paradigm if the fitting explained better the data than chance (*F* test, *P* = 0.05). Unresponsive neurons were considered as having zero amplitude of modulation and no phase value (i.e., their phase was not considered for further analysis). A preferred directional tuning for each neuron was obtained by fitting a cosine function to their neuronal responses to vestibular stimulation along different azimuths (*SI Appendix, Fig. S3*).

PCs were classified as translation-only, tilt-only, GIA-only, and complex neurons according to the computational model that best explained their SS responses to our tilt/translation stimulation protocol at 1-Hz stimulation and at the azimuth orientation that provided the largest neuronal response to translation and tilt-translation paradigms.

Description of Computational Models. We describe PC SS responses using several linear models; namely, translation model, tilt model, GIA model, and complex models. These models assume that neuronal responses can be explained by changes in “*g*” forces and tilt angle as follows (also see *SI Appendix, Methods and Fig. S6* for further details).

We use sinusoidal functions to represent the different stimuli (translation, tilt, and GIA) during each paradigm (see stimulus traces in *SI Appendix, Fig. S6A*). Assuming that PC responses are linearly related to these stimuli (see refs. 15, 21, 24), their neuronal discharge can also be described by sinusoidal functions. For example, the estimated output of the “translation-only” model during a particular paradigm corresponds to a sinusoidal function representing the translation “stimulus” scaled by a factor, which is the gain of the translation component, and a delay or phase shift, which corresponds to the phase of the translation component. In the case of complex models, the estimated output corresponds to the sum of two or more sinusoidal functions, each one related to specific input signals (translation, tilt, and GIA) multiplied by their own gain and phase. Therefore, the function used to fit the experimental data for all paradigms (i.e., translation, tilt, tilt-translation, and tilt+translation) is as follows:

$$f(t) = \sum_{\text{Comp}} G_{\text{Comp}} \times A_{\text{Comp}} \times \sin(2\pi\nu t + \theta_{\text{Comp}} + \delta_{\text{Comp}}) + DC,$$

where the summatory is extended to the different components (Comp) belonging to a particular model (e.g., the translation model has only the translation component, while the complex model with tilt and translation has both translation and tilt components). G_{Comp} and δ_{Comp} are the gain and the phase shift ascribed to the response of each component, and A_{Comp} and θ_{Comp} are the amplitude and the phase of the corresponding stimuli (e.g., the translation stimuli for the translation component). DC is the resting firing rate of the neuron, and $\nu = 1$ Hz is the frequency.

The experimental data were fitted to this function using a least-square fitting method [we use Nelder-Mead algorithm (68)] to find the values of our design variables (*SI Appendix, Fig. S6*; e.g., gain and phase of the translation component). To ensure we find the global minimum, we run this optimization method starting at different initial values for the design variables.

The performance of different models was evaluated by comparing their residuals using *F* statistics (*P* = 0.05). We classified neurons as GIA-only, tilt-only, translation-only, or complex, to reflect the model that explains significantly better the data than other models while using the lowest number of components. For example, a PC that shows similar fitting performance for complex and translation models and significantly worst fitting for the remaining models would be classified as translation-only PC.

From the model fit, we obtained the variance accounted for (VAF) for each neuron. This VAF was subsequently normalized (VAF*) as the percentage value of the best possible VAF. The best possible VAF was obtained from fitting neuronal responses to each paradigm with independent sinusoidal functions. This fitting method assumes “no a priori relationship” between the neuronal response to different vestibular paradigms (16). The only assumption is that neuronal responses can be approximated by 1-Hz sinusoidal functions. The advantage of using the VAF* instead of the VAF is that it

allows a comparison of neuronal responses regardless of their firing irregularity and the number of cycles used for averaging.

The above computational model could not be reliably applied to investigate the information carried by CS responses because of the low number of data points available to estimate the goodness of the fit. This low number of data points is a consequence of the large bin size used to construct CS PSTHs (0.1 s) and the presence of zero cutoff in CS responses. Therefore, we tackled the question of what information is encoded in CS responses indirectly—we compared CS and SS responses within the same PC during each of the tilt/translation paradigms, as shown in *SI Appendix, Fig. S5*.

1. D. E. Angelaki, T. A. Yakusheva, A. M. Green, J. D. Dickman, P. M. Blazquez, Computation of egomotion in the macaque cerebellar vermis. *Cerebellum* **9**, 174–182 (2010).
2. B. L. McNaughton, F. P. Battaglia, O. Jensen, E. I. Moser, M. B. Moser, Path integration and the neural basis of the “cognitive map.”. *Nat. Rev. Neurosci.* **7**, 663–678 (2006).
3. J. D. Dickman, D. E. Angelaki, M. J. Correia, Response properties of gerbil otolith afferents to small angle pitch and roll tilts. *Brain Res.* **556**, 303–310 (1991).
4. C. Fernández, J. M. Goldberg, Physiology of peripheral neurons innervating otolith organs of the squirrel monkey. I. Response to static tilts and to long-duration centrifugal force. *J. Neurophysiol.* **39**, 970–984 (1976).
5. D. E. Angelaki, M. Q. McHenry, J. D. Dickman, S. D. Newlands, B. J. Hess, Computation of inertial motion: Neural strategies to resolve ambiguous otolith information. *J. Neurosci.* **19**, 316–327 (1999).
6. A. M. Green, D. E. Angelaki, An integrative neural network for detecting inertial motion and head orientation. *J. Neurophysiol.* **92**, 905–925 (2004).
7. A. M. Green, A. G. Shaikh, D. E. Angelaki, Sensory vestibular contributions to constructing internal models of self-motion. *J. Neural Eng.* **2**, S164–S179 (2005).
8. R. G. Heath, J. W. Harper, Ascending projections of the cerebellar fastigial nucleus to the hippocampus, amygdala, and other temporal lobe sites: Evoked potential and histological studies in monkeys and cats. *Exp. Neurol.* **45**, 268–287 (1974).
9. W. Liu, Y. Zhang, W. Yuan, J. Wang, S. Li, A direct hippocampo-cerebellar projection in chicken. *Anat. Rec.* **295**, 1311–1320 (2012).
10. A. Arrigo *et al.*, Constrained spherical deconvolution analysis of the limbic network in human, with emphasis on a direct cerebello-limbic pathway. *Front. Hum. Neurosci.* **8**, 987 (2014).
11. W. Yu, E. Krook-Magnuson, Cognitive collaborations: Bidirectional functional connectivity between the cerebellum and the hippocampus. *Front. Syst. Neurosci.* **9**, 177 (2015).
12. N. H. Barmack, R. W. Baughman, P. Errico, H. Shojaku, Vestibular primary afferent projection to the cerebellum of the rabbit. *J. Comp. Neurol.* **327**, 521–534 (1993).
13. N. H. Barmack, Central vestibular system: Vestibular nuclei and posterior cerebellum. *Brain Res. Bull.* **60**, 511–541 (2003).
14. S. D. Newlands *et al.*, Central projections of the saccular and utricular nerves in macaques. *J. Comp. Neurol.* **466**, 31–47 (2003).
15. T. A. Yakusheva *et al.*, Purkinje cells in posterior cerebellar vermis encode motion in an inertial reference frame. *Neuron* **54**, 973–985 (2007).
16. J. Laurens, H. Meng, D. E. Angelaki, Neural representation of orientation relative to gravity in the macaque cerebellum. *Neuron* **80**, 1508–1518 (2013).
17. E. Burguière *et al.*, Spatial navigation impairment in mice lacking cerebellar LTD: A motor adaptation deficit? *Nat. Neurosci.* **8**, 1292–1294 (2005).
18. C. Rochefort *et al.*, Cerebellum shapes hippocampal spatial code. *Science* **334**, 385–389 (2011).
19. C. I. De Zeeuw *et al.*, Expression of a protein kinase C inhibitor in Purkinje cells blocks cerebellar LTD and adaptation of the vestibulo-ocular reflex. *Neuron* **20**, 495–508 (1998).
20. L. Rondi-Reig, A. L. Paradis, J. M. Lefort, B. M. Babayan, C. Tobin, How the cerebellum may monitor sensory information for spatial representation. *Front. Syst. Neurosci.* **8**, 205 (2014).
21. D. E. Angelaki, A. G. Shaikh, A. M. Green, J. D. Dickman, Neurons compute internal models of the physical laws of motion. *Nature* **430**, 560–564 (2004).
22. A. M. Green, H. Meng, D. E. Angelaki, A reevaluation of the inverse dynamic model for eye movements. *J. Neurosci.* **27**, 1346–1355 (2007).
23. H. Meng, P. M. Blázquez, J. D. D. Dickman, D. E. Angelaki, Diversity of vestibular nuclei neurons targeted by cerebellar nodulus inhibition. *J. Physiol.* **592**, 171–188 (2014).
24. T. Yakusheva, P. M. Blázquez, D. E. Angelaki, Frequency-selective coding of translation and tilt in macaque cerebellar nodulus and uvula. *J. Neurosci.* **28**, 9997–10009 (2008).
25. V. Yakhnitsa, N. H. Barmack, Antiphasic Purkinje cell responses in mouse uvula-nodulus are sensitive to static roll-tilt and topographically organized. *Neuroscience* **143**, 615–626 (2006).
26. A. Badura *et al.*, Climbing fiber input shapes reciprocity of Purkinje cell firing. *Neuron* **78**, 700–713 (2013).
27. M. M. ten Brinke *et al.*, Evolving models of Pavlovian conditioning: Cerebellar cortical dynamics in awake behaving mice. *Cell Rep.* **13**, 1977–1988 (2015).
28. J. S. Albus, A theory of cerebellar function. *Math. Biosci.* **10**, 25–61 (1971).
29. P. Dean, J. Porrill, C. F. Ekerot, H. Jörnell, The cerebellar microcircuit as an adaptive filter: Experimental and computational evidence. *Nat. Rev. Neurosci.* **11**, 30–43 (2010).
30. J. C. Eccles, M. Ito, J. Szentagothai, *The Cerebellum as a Neuronal Machine*, J. C. Eccles, L. Provini, P. Strat, H. Taborikova, Eds. (Springer, 1967), pp. 171–194.
31. D. Marr, A theory of cerebellar cortex. *J. Physiol.* **202**, 437–470 (1969).
32. J. F. Medina, M. D. Mauk, Computer simulation of cerebellar information processing. *Nat. Neurosci.* **3** (suppl.), 1205–1211 (2000).
33. P. M. Blázquez, T. A. Yakusheva, GABA-A inhibition shapes the spatial and temporal response properties of Purkinje cells in the macaque cerebellum. *Cell Rep.* **11**, 1043–1053 (2015).
34. S. J. Mitchell, R. A. Silver, Shunting inhibition modulates neuronal gain during synaptic excitation. *Neuron* **38**, 433–445 (2003).
35. T. L. Stay, J. Laurens, R. V. Sillitoe, D. E. Angelaki, Genetically eliminating Purkinje neuron GABAergic neurotransmission increases their response gain to vestibular motion. *Proc. Natl. Acad. Sci. U.S.A.* **116**, 3245–3250 (2019).
36. P. Wulff *et al.*, Synaptic inhibition of Purkinje cells mediates consolidation of vestibulo-cerebellar motor learning. *Nat. Neurosci.* **12**, 1042–1049 (2009).
37. F. J. Geurts, E. De Schutter, S. Dieudonné, Unraveling the cerebellar cortex: Cytology and cellular physiology of large-sized interneurons in the granular layer. *Cerebellum* **2**, 290–299 (2003).
38. E. Mugnaini, A. Floris, The unipolar brush cell: A neglected neuron of the mammalian cerebellar cortex. *J. Comp. Neurol.* **339**, 174–180 (1994).
39. E. Mugnaini, G. Sekerková, M. Martina, The unipolar brush cell: A remarkable neuron finally receiving deserved attention. *Brain Res. Brain Res. Rev.* **66**, 220–245 (2011).
40. J. Laurens, S. A. Heiney, G. Kim, P. M. Blázquez, Cerebellar cortex granular layer interneurons in the macaque monkey are functionally driven by mossy fiber pathways through net excitation or inhibition. *PLoS One* **8**, e82239 (2013).
41. C. V. Rousseau *et al.*, Mixed inhibitory synaptic balance correlates with glutamatergic synaptic phenotype in cerebellar unipolar brush cells. *J. Neurosci.* **32**, 4632–4644 (2012).
42. J. M. Lefort *et al.*, Impaired cerebellar Purkinje cell potentiation generates unstable spatial map orientation and inaccurate navigation. *Nat. Commun.* **10**, 2251 (2019).
43. T. Yamazaki, S. Nagao, A computational mechanism for unified gain and timing control in the cerebellum. *PLoS One* **7**, e33319 (2012).
44. H. J. Boele *et al.*, Impact of parallel fiber to Purkinje cell long-term depression is unmasked in absence of inhibitory input. *Sci. Adv.* **4**, s9426 (2018).
45. S. K. Koekkoek, W. L. Den Ouden, G. Perry, S. M. Highstein, C. I. De Zeeuw, Monitoring kinetic and frequency-domain properties of eyelid responses in mice with magnetic distance measurement technique. *J. Neurophysiol.* **88**, 2124–2133 (2002).
46. C. I. De Zeeuw, D. R. Wylie, J. S. Stahl, J. I. Simpson, Phase relations of Purkinje cells in the rabbit flocculus during compensatory eye movements. *J. Neurophysiol.* **74**, 2051–2064 (1995).
47. A. E. Luebke, D. A. Robinson, Gain changes of the cat’s vestibulo-ocular reflex after flocculus deactivation. *Exp. Brain Res.* **98**, 379–390 (1994).
48. A. Mizukoshi *et al.*, Motor dynamics encoding in the rostral zone of the cat cerebellar flocculus during vertical optokinetic eye movements. *Exp. Brain Res.* **132**, 260–268 (2000).
49. J. I. Simpson, T. Belton, M. Suh, B. Winkelman, Complex spike activity in the flocculus signals more than the eye can see. *Ann. N. Y. Acad. Sci.* **978**, 232–236 (2002).
50. L. S. Stone, S. G. Lisberger, Visual responses of Purkinje cells in the cerebellar flocculus during smooth-pursuit eye movements in monkeys. I. Simple spikes. *J. Neurophysiol.* **63**, 1241–1261 (1990).
51. T. Yakusheva, P. M. Blázquez, D. E. Angelaki, Relationship between complex and simple spike activity in macaque caudal vermis during three-dimensional vestibular stimulation. *J. Neurosci.* **30**, 8111–8126 (2010).
52. H. H. Goossens *et al.*, Simple spike and complex spike activity of floccular Purkinje cells during the optokinetic reflex in mice lacking cerebellar long-term depression. *Eur. J. Neurosci.* **19**, 687–697 (2004).
53. S. J. Blakemore, D. M. Wolpert, C. D. Frith, Central cancellation of self-produced tickle sensation. *Nat. Neurosci.* **1**, 635–640 (1998).
54. J. X. Brooks, K. E. Cullen, The primate cerebellum selectively encodes unexpected self-motion. *Curr. Biol.* **23**, 947–955 (2013).
55. T. J. Ebner, S. Pasalar, Cerebellum predicts the future motor state. *Cerebellum* **7**, 583–588 (2008).
56. R. C. Miall, D. J. Weir, D. M. Wolpert, J. F. Stein, Is the cerebellum a Smith predictor? *J. Mot. Behav.* **25**, 203–216 (1993).
57. L. S. Popa, T. J. Ebner, Cerebellum, predictions and errors. *Front. Cell. Neurosci.* **12**, 524 (2019).

58. J. Stein, Cerebellar forward models to control movement. *J. Physiol.* **587**, 299 (2009).
59. D. M. Wolpert, R. C. Miall, M. Kawato, Internal models in the cerebellum. *Trends Cogn. Sci.* **2**, 338–347 (1998).
60. A. M. van Alphen, C. I. De Zeeuw, Cerebellar LTD facilitates but is not essential for long-term adaptation of the vestibulo-ocular reflex. *Eur. J. Neurosci.* **16**, 486–490 (2002).
61. S. K. Koekkoek *et al.*, Cerebellar LTD and learning-dependent timing of conditioned eyelid responses. *Science* **301**, 1736–1739 (2003).
62. J. Goossens *et al.*, Expression of protein kinase C inhibitor blocks cerebellar long-term depression without affecting Purkinje cell excitability in alert mice. *J. Neurosci.* **21**, 5813–5823 (2001).
63. R. Apps *et al.*, Cerebellar modules and their role as operational cerebellar processing units: A consensus paper [Corrected]. *Cerebellum* **17**, 654–682 (2018).
64. T. J. Ruigrok, A. Pijpers, E. Goedknegt-Sabel, P. Coulon, Multiple cerebellar zones are involved in the control of individual muscles: A retrograde trans-neuronal tracing study with rabies virus in the rat. *Eur. J. Neurosci.* **28**, 181–200 (2008).
65. M. Schonewille *et al.*, Reevaluating the role of LTD in cerebellar motor learning. *Neuron* **70**, 43–50 (2011).
66. W. Kakegawa *et al.*, Optogenetic control of synaptic AMPA receptor endocytosis reveals roles of LTD in motor learning. *Neuron* **99**, 985–998.e6 (2018).
67. R. A. Hensbroek *et al.*, Identifying Purkinje cells using only their spontaneous simple spike activity. *J. Neurosci. Methods* **232**, 173–180 (2014).
68. J. C. Lagarias, J. A. Reeds, M. H. Wright, P. E. Wright, Convergence properties of the Nelder-Mead simplex method in low dimensions. *SIAM J. Optim.* **9**, 112–147 (1998).